

## Synthesis, Characterization, and Theoretical Study of Some New Organotellurium Compounds Derived from Camphor

Nuha Hussain Al-Saadawy\*

Department of Chemistry, College of Science, University of Thi-Qar, Thi-Qar, Iraq

\* Corresponding author:

email: nuh.hussain@sci.utq.ed.iq

Received: October 15, 2021

Accepted: November 26, 2021

DOI: 10.22146/ijc.69805

**Abstract:** The present work describes the synthesis of a variety of organotellurium compounds. The first part describes the synthesis of a new series of organotellurium compounds containing azomethine groups. Reaction of (E)-(4-((1,7,7-trimethyl bicyclo[2.2.1]heptan-2-ylidene)amino)phenyl)mercury(II)chloride and (E)-(5-methyl-2-((1,7,7-trimethylbicyclo[2.2.1]heptan-2-ylidene)amino)phenyl) mercury(II)chloride with tellurium tetrabromide in 2:1 mole ratio yielded the tellurated Schiff bases  $Ar_2TeBr_2$  (where  $Ar = 1-(C_9H_{16}C=N)C=N)C_6H_4$  and  $1-(C_9H_{16}C=N)C=N)-4-CH_3C_6H_3$ ) respectively. Reduction of organyl tellurium dibromide  $Ar_2TeBr_2$  by hydrazine hydrate obtained the corresponding tellurides (i.e.,  $Ar_2Te$ ) in good yields. Characterization of the prepared compounds was carried out using infrared spectrum (FT-IR), proton nuclear magnetic resonance spectrum ( $^1H$ -NMR), and elemental analysis (CHN). The molecular structure of the organotellurium compounds was investigated using the density functional theory with hybrid functional (B3LYP), and the basis set 6-31G Geometrical structure, HOMO surfaces, LUMO surfaces, and energy gap have been produced throughout the geometry optimization. The molecular geometry and contours for the organotellurium compounds were investigated throughout the geometrical optimization. The donor and acceptor properties have been studied by comparing organotellurium compounds' highest occupied molecular orbital energies (HOMO). The present study aims to prepare organotellurium compounds derived from aniline, p-toluidine, and camphor and their derivatives using tellurated Schiff bases.

**Keywords:** organotellurium; telluride; organyl tellurium dibromide; HOMO and LUMO energies; camphor; density functional theory

### ■ INTRODUCTION

In recent years, there has been a great deal of interest in synthesizing organotellurium compounds containing amino [1-2], azomethine [3], pyridines, or acetamido group in 2-position of tellurium element [1]. The high stability of such compounds is due to the intramolecular interactions ( $N \rightarrow Te$ ). There are few examples of tellurated derivatives of azobenzenes in the literature, although the first example was prepared in 1979 by trans-metallation of mercurated azobenzenes with tellurium tetrachloride [4-6]. In the last ten years, the field of organic tellurium chemistry has witnessed a vast development, and several review articles and books on the subject have been published [3,7-11]. Organotellurium compounds have

long proved to be valuable intermediate products in organic synthesis, are known to be convenient models for studying fundamental problems of theoretical chemistry, and are essential substances from the practical viewpoint [12-13]. Elemental tellurium provides a source of nucleophilic (chalcogenide and dichalcogenide ions) and electrophilic reagents, which may be generated in situ or prepared just before use [14-15]. Elemental tellurium can be brought into insertion reaction with organometallic compounds to afford the corresponding metal tellurolates, which are then involved in nucleophilic substitution and addition reactions [15]. Organotellurium compounds have been used as precursors for the preparative organic synthesis

and semiconducting metal tellurides. Organotellurium chemistry has become a trending topic [5,7-9,16].

The quantum mechanical wave function contains all the information about the given system [17]. In the case of a simple 2-D square potential or even a hydrogen atom, the Schrodinger equation may be solved to get the system's wave function, following which the allowed energy states of the system can be determined [11]. The simplest definition of density functional theory (DFT) is a technique used to approximate the Schrödinger equation of many-body systems [18]. Computational codes refer to DFT in the Gaussian 09 program. DFT is one of the most common methods of quantum mechanics. DFT exactly describes the rigid structure of the molecules throughout the geometrical optimization procedure. In application, it is used to investigate the structural, electronic, and physical properties of the molecules and materials, such as the binding energies of the molecules in chemistry, physics, and other areas [[19]]. For example, DFT aims to calculate the electronic ground state energy of a system of N electrons only through its density without prior well-known system wave function [11,17,18,20-23].

In the present work, attempts will be made to prepare several new organotellurium compounds containing group ( $-C=N$ ). However, to the best of our knowledge, there is no method to prepare organotellurium compounds derived from camphor, aniline, and *p*-toluidine. Therefore, the current study aims at studying the biological activity of these new compounds.

## ■ EXPERIMENTAL SECTION

### Materials

The chemicals used in this study included camphor, ethanol absolute, *p*-toluidine, glacial acetic acid, mercuric acetate, bromine, chloroform, dioxane, sodium metal, potassium hydroxide, hydrazine hydrate, aniline (Avantor), lithium chloride, tellurium powder, hydrochloric acid (HGB), and molecular sieves (ACS). All the chemicals in this study were used as obtained by the manufacturer with no further purification.

### Instrumentation

The  $^1\text{H-NMR}$  spectra were recorded on Bruker 500 MHz spectrometers with TMS as an internal reference, utilizing soluble  $\text{DMSO-}d_6$ . Elemental analysis for carbon, hydrogen, and nitrogen was performed using a Euro vector EA 3000A Elemental Analysis (Italy). Infrared spectra were recorded with KBr circles, utilizing an FTIR spectrophotometer Shimadzu model 8400 S in  $4000\text{--}250\text{ cm}^{-1}$ . This study begins by optimizing A, B, C, and D compounds using the DFT method, implemented in the Gaussian 09W package with the 6-31G basis set in its ground state. Depending on the first principle of DFT computations, the energy gaps ( $E_g$ ) and frontier orbital distributions (HOMO and LUMO) are computed for all these systems. DFT using Becke and Lee-Yang-Parr exchange-correlation functional, with the 6-31G mention basis set were applied in the quantum-chemical evaluation.

### Procedure

#### **Synthesis of (2E,2'E)-N,N'-((dibromo- $\lambda^4$ -tellanediyl)bis(4,1-phenylene))bis(1,7,7-trimethylbicyclo[2.2.1]heptan-2-imine) (A)**

Firstly, (5.5 mmol, 2.54 g) of (E)-(4-((1,7,7-trimethylbicyclo[2.2.1]heptan-2-ylidene)amino) phenyl) mercury(II) chloride was dissolved in 25 mL of dry dioxane. Then, (2.8 mmol, 1.25 g) of tellurium tetrabromide in 25 mL of dry dioxane was added to the mixture. The mixture was then refluxed for 14 h, the hot solution was filtered, and the filtrate was cooled to room temperature [1-2,11]. The filtrate was poured into 250 mL of cold distilled water to form reddish-brown crystals. Following recrystallization by ethanol, brown crystals were formed, yielding 63% and melting point  $103\text{--}105\text{ }^\circ\text{C}$ .

C.H.N.: theoretical % (practical %): C, 51.93 (51.64); H, 5.45 (5.33); N, 3.79 (3.47); FT-IR using KBr:  $\nu(\text{C-H})$  Aliphatic =  $3100\text{ cm}^{-1}$ ,  $\nu(\text{C-H})$  Aromatic =  $3194\text{ cm}^{-1}$ ,  $\nu(\text{C=N})$  Aliphatic =  $1679\text{ cm}^{-1}$ ,  $\nu(\text{C=N})$  Aromatic =  $1325\text{ cm}^{-1}$ ,  $\nu(\text{C=C})$  Aromatic =  $1404\text{ cm}^{-1}$ .

$^1\text{H-NMR}$  (500 MHz,  $\text{DMSO-}d_6$ )  $\delta$  6.97 (s, 6H), 6.81 (d,  $J = 7.9\text{ Hz}$ , 4H), 6.78–6.72 (m, 8H), 6.55 (d,  $J = 8.0\text{ Hz}$ , 6H), 6.51 (s, 1H), 6.47 (d,  $J = 8.0\text{ Hz}$ , 3H), 3.75 (dd,

$J = 10.6, 3.6$  Hz, 8H), 2.74 (dd,  $J = 16.0, 10.6$  Hz, 8H), 2.47 (d,  $J = 3.6$  Hz, 6H), 2.11 (d,  $J = 12.8$  Hz, 24H), 2.07 (s, 7H). These data were shown in Scheme 1, Table 1 and 2, Fig. S1, S2 and S9.

### Synthesis of (2*E*,2'*E*)-*N,N'*-(tellurobis(4,1-phenylene))bis(1,7,7-trimethylbicyclo[2.2.1]heptan-2-imine) (B)

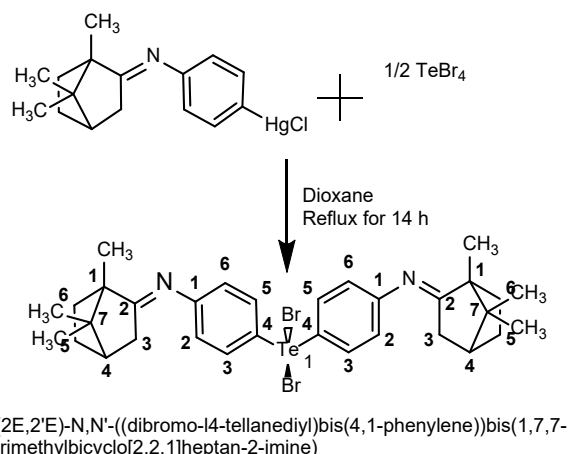
(2*E*,2'*E*)-*N,N'*-((dibromo- $\lambda^4$ -tellanediy)bis(4,1-phenylene))bis(1,7,7-trimethylbicyclo[2.2.1]heptan-2-imine) (5 mmol, 3.7 g) was dissolved in 25 mL of ethanol. The solution was then refluxed for 2 h, and the mixture was cooled to room temperature. To the mixture, hydrazine hydrate (5 mmol, 0.16 g) in 25 mL of ethanol was added dropwise and heated in the water bath to 70 °C. The resulting solution was evaporated using a rotary evaporator [1-2,11]. The brown solid that had formed was recrystallized by using chloroform to give brown crystals, with a yield of 55%, and melting point 88–90 °C.

C.H.N: theoretical % (practical %): C, 66.23 (66.45); H, 6.95 (6.83); N, 4.83 (4.11); FT-IR using KBr:  $\nu(\text{C-H})$  Aliphatic = 2920  $\text{cm}^{-1}$ ,  $\nu(\text{C-H})$  Aromatic = 3103  $\text{cm}^{-1}$ ,  $\nu(\text{C=N})$  Aliphatic = 1616  $\text{cm}^{-1}$ ,  $\nu(\text{C-N})$  Aromatic = 1333  $\text{cm}^{-1}$ ,  $\nu(\text{C=C})$  Aromatic = 1419  $\text{cm}^{-1}$ .

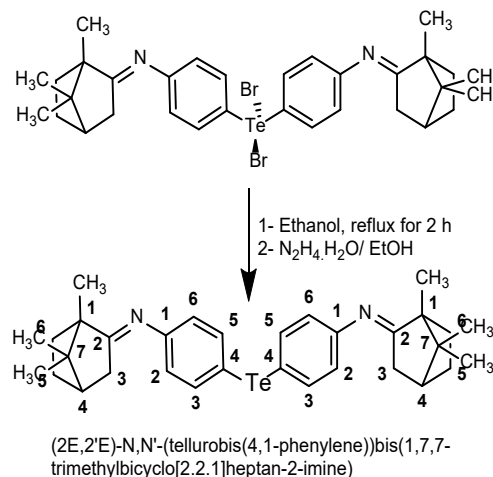
$^1\text{H-NMR}$  (500 MHz,  $\text{DMSO-}d_6$ )  $\delta$  6.97 (s, 6H), 6.81 (d,  $J = 7.9$  Hz, 4H), 6.78–6.72 (m, 8H), 6.55 (d,  $J = 8.0$  Hz, 6H), 6.51 (s, 1H), 6.47 (d,  $J = 8.0$  Hz, 3H), 3.75 (dd,  $J = 10.6, 3.6$  Hz, 8H), 2.74 (dd,  $J = 16.0, 10.6$  Hz, 8H), 2.47 (d,  $J = 3.6$  Hz, 6H), 2.11 (d,  $J = 12.8$  Hz, 24H), 2.07 (s, 7H). These data were shown in Scheme 2, Table 1 and 2, Fig. S3, S4, and S10.

### Synthesis of (E)-*N*-(2-(dibromo(5-methyl-2-((E)-1,7,7-trimethylbicyclo[2.2.1]heptan-2-ylidene)amino)phenyl)- $\lambda^4$ -tellaneyl)-4-methylphenyl)-1,7,7-trimethylbicyclo[3.1.1]heptan-6-imine (C)

(E)-5-methyl-2-((1,7,7-trimethylbicyclo[2.2.1]heptan-2-ylidene)amino)phenylmercury(II) chloride (5.5 mmol, 2.62 g) was dissolved in 25 mL of dry dioxane. To the solution, (2.8 mmol, 1.25 g) of tellurium tetrabromide in 25 mL of dry dioxane was added and then refluxed for 14 h. Next, the hot solution was filtered, and the filtrate was cooled to room temperature [1-2,11]. The filtrate was poured into 250 mL of cold distilled water to form brown crystals, recrystallization by ethanol to give



**Scheme 1.** Preparation of diorganyl tellurium dibromide of aniline and camphor derivative

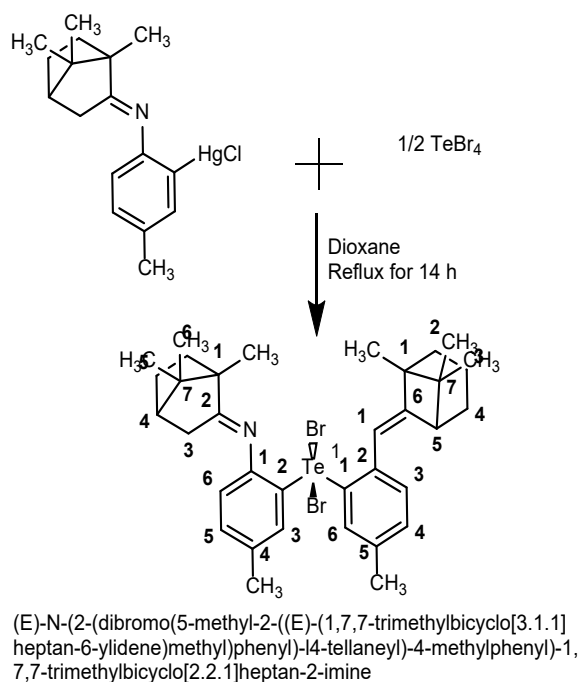


**Scheme 2.** Preparation of diorganyl telluride of aniline and camphor derivative

brown crystals, with a yield of 65%, and melting point 123–125 °C.

C.H.N: theoretical % (practical %): C, 53.16 (52.95); H, 5.77 (5.45); N, 3.79 (3.47); FT-IR using KBr:  $\nu(\text{C-H})$  Aliphatic = 2951  $\text{cm}^{-1}$ ,  $\nu(\text{C-H})$  Aromatic = 2999  $\text{cm}^{-1}$ ,  $\nu(\text{C=N})$  Aliphatic = 1694  $\text{cm}^{-1}$ ,  $\nu(\text{C-N})$  Aromatic = 1396  $\text{cm}^{-1}$ ,  $\nu(\text{C=C})$  Aromatic = 1487  $\text{cm}^{-1}$ .

$^1\text{H-NMR}$  (500 MHz,  $\text{DMSO-}d_6$ )  $\delta$  7.93 (d,  $J = 7.8$  Hz, 8H), 7.89 (s, 1H), 7.78 (dt,  $J = 26.1, 7.7$  Hz, 7H), 7.64 (t,  $J = 7.6$  Hz, 10H), 7.60–7.44 (m, 3H), 7.02 (dd,  $J = 24.2, 8.0$  Hz, 2H), 6.67 (d,  $J = 8.0$  Hz, 1H), 2.16 (s, 1H). These data were shown in Scheme 3, Table 1 and 2, Fig. S5, S6, and S11.



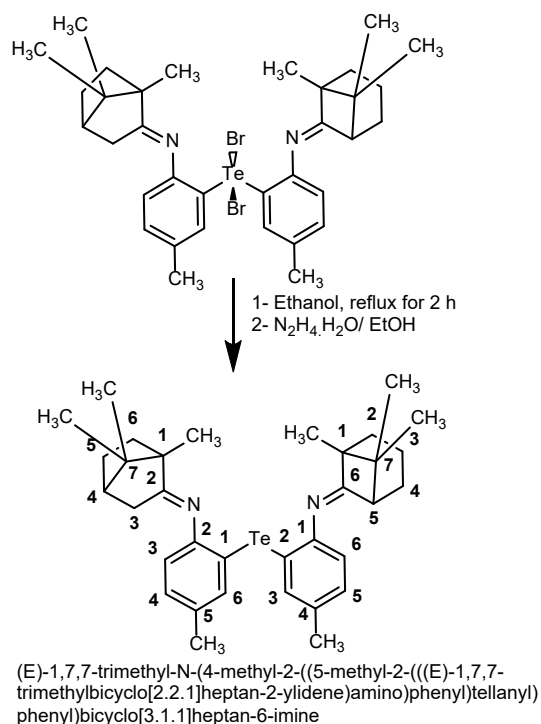
**Scheme 3.** Preparation of diorganyl tellurium dibromide of *p*-toluidine and a camphor derivative

**Synthesis of (E)-1,7,7-trimethyl-N-(4-methyl-2-((5-methyl-2-(((E)-1,7,7-trimethylbicyclo[2.2.1]heptan-2-ylidene)amino)phenyl)tellanyl)phenyl)bicyclo[3.1.1]heptan-6-imine (D)**

(E)-N-(2-(dibromo(5-methyl-2-((E)-(1,7,7-trimethylbicyclo[3.1.1]heptan-6-ylidene)methyl)phenyl)-4-tellanyl)-4-methylphenyl)-1,7,7-trimethylbicyclo[2.2.1]heptan-2-imine (5 mmol., 3.8 g) was dissolved in 25 mL of ethanol. Then, the solution was refluxed for 2 h, and the mixture was cooled to room temperature. To the mixture, hydrazine hydrate (5 mmol., 0.16 g) in 25 mL of ethanol was added dropwise and heated in a water bath to 70 °C. The resulting solution was evaporated using a rotary evaporator. The brown solid that had formed was recrystallized by using chloroform to give brown crystals [1,2,11], with a yield of 51%, melting point of 95–97 °C.

C.H.N: theoretical % (practical %): C, 67.13 (66.98); H, 7.29 (7.13); N, 4.60 (4.83); FT-IR using KBr:  $\nu(\text{C-H})$  Aliphatic = 2951  $\text{cm}^{-1}$ ,  $\nu(\text{C-H})$  Aromatic = 2998  $\text{cm}^{-1}$ ,  $\nu(\text{C=N})$  Aliphatic = 1692  $\text{cm}^{-1}$ ,  $\nu(\text{C-N})$  Aromatic = 1394  $\text{cm}^{-1}$ ,  $\nu(\text{C=C})$  Aromatic = 1487  $\text{cm}^{-1}$ .

$^1\text{H-NMR}$  (500 MHz, DMSO- $d_6$ )  $\delta$  7.93 (d,  $J = 7.7$  Hz, 1H), 7.78 (td,  $J = 16.0, 15.5, 7.6$  Hz, 3H), 7.55 (ddt,  $J = 54.8,$



**Scheme 4.** Preparation of diorganyl telluride of *p*-toluidine and a camphor derivative

22.5, 7.6 Hz, 5H), 6.99 (d,  $J = 7.9$  Hz, 1H), 6.76 (d,  $J = 7.9$  Hz, 1H), 2.15 (s, 2H). These data were shown in Scheme 4, Table 1 and 2, Fig. S7, S8, and S12.

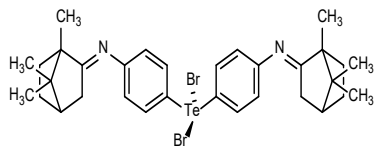
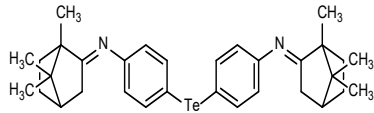
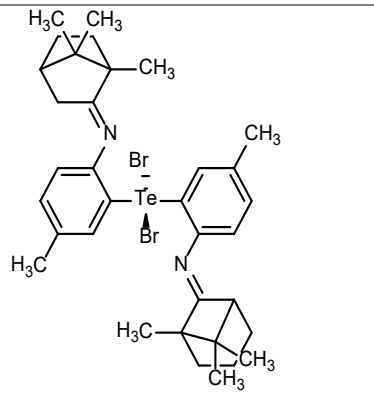
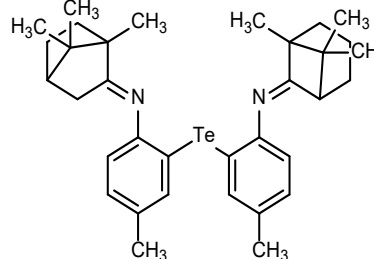
## RESULTS AND DISCUSSION

The present work included the preparation of organotellurium compounds such as  $\text{Ar}_2\text{TeBr}_2$  and  $\text{Ar}_2\text{Te}$  (where  $\text{Ar} = 1-(\text{C}_9\text{H}_{16}\text{C}=\text{N})\text{C}=\text{N})\text{C}_6\text{H}_4$  and  $1-(\text{C}_9\text{H}_{16}\text{C}=\text{N})\text{C}=\text{N})-4-\text{CH}_3\text{C}_6\text{H}_3$ , respectively) by tellurated Schiff base derived of camphor, aniline, and *p*-toluidine.

$^1\text{H-NMR}$  spectra of compounds (A–D) showed all the expected peaks. All spectrum [16,24–28] in DMSO- $d_6$  are given in Table 1 and explained in Fig. S1–S8.

IR spectra of the compounds under study displayed standard features in specific regions and characteristic bands in the other areas [24–29] (explained in Table 2). In all the compounds under study, the aromatic (C–H) bond appeared at the range (2998–3194  $\text{cm}^{-1}$ ) [24–29], whereas the aliphatic (C–H) bond appeared at the range of (2920–3100  $\text{cm}^{-1}$ ). The clear band at the range of (1616–1696  $\text{cm}^{-1}$ ) was attributed to the aliphatic bond (C=N) [24–29]. On the

**Table 1.** <sup>1</sup>H-NMR spectral data of selected compounds

Structure for compound	<sup>1</sup> H-NMR (DMSO- <i>d</i> <sub>6</sub> ); TMS = 0 ppm
<p>A</p> 	6.97 (s, 6H), 6.81 (d, <i>J</i> = 7.9 Hz, 4H), 6.78–6.72 (m, 8H), 6.55 (d, <i>J</i> = 8.0 Hz, 6H), 6.51 (s, 1H), 6.47 (d, <i>J</i> = 8.0 Hz, 3H), 3.75 (dd, <i>J</i> = 10.6, 3.6 Hz, 8H), 2.74 (dd, <i>J</i> = 16.0, 10.6 Hz, 8H), 2.47 (d, <i>J</i> = 3.6 Hz, 6H), 2.11 (d, <i>J</i> = 12.8 Hz, 24H), 2.07 (s, 7H)
<p>B</p> 	6.97 (s, 6H), 6.81 (d, <i>J</i> = 7.9 Hz, 4H), 6.78–6.72 (m, 8H), 6.55 (d, <i>J</i> = 8.0 Hz, 6H), 6.51 (s, 1H), 6.47 (d, <i>J</i> = 8.0 Hz, 3H), 3.75 (dd, <i>J</i> = 10.6, 3.6 Hz, 8H), 2.74 (dd, <i>J</i> = 16.0, 10.6 Hz, 8H), 2.47 (d, <i>J</i> = 3.6 Hz, 6H), 2.11 (d, <i>J</i> = 12.8 Hz, 24H), 2.07 (s, 7H)
<p>C</p> 	7.93 (d, <i>J</i> = 7.8 Hz, 8H), 7.89 (s, 1H), 7.78 (dt, <i>J</i> = 26.1, 7.7 Hz, 7H), 7.64 (t, <i>J</i> = 7.6 Hz, 10H), 7.60–7.44 (m, 3H), 7.02 (dd, <i>J</i> = 24.2, 8.0 Hz, 2H), 6.67 (d, <i>J</i> = 8.0 Hz, 1H), 2.16 (s, 1H)
<p>D</p> 	7.93 (d, <i>J</i> = 7.7 Hz, 1H), 7.78 (td, <i>J</i> = 16.0, 15.5, 7.6 Hz, 3H), 7.55 (ddt, <i>J</i> = 54.8, 22.5, 7.6 Hz, 5H), 6.99 (d, <i>J</i> = 7.9 Hz, 1H), 6.76 (d, <i>J</i> = 7.9 Hz, 1H), 2.15 (s, 2H)

**Table 2.** FT-IR spectral data of selected compounds

Compound	Aromatic	Aliphatic	Aliphatic	Aromatic	Aromatic
	C–H	C–H	C=N	C–N	C=C
A	3194	3100	1679	1325	1404
B	3103	2920	1616	1333	1419
C	2999	2951	1694	1396	1487
D	2998	2951	1692	1394	1487

other hand, the band at the range of 1325–1396 cm<sup>-1</sup> was attributed to the aromatic (C–N) bond for all the prepared compounds. The aromatic (C=C) bond appeared at the range of (1404–1487 cm<sup>-1</sup>) [24–29], as shown in Table 2 and Fig. S9–S12.

### Computational Study

The molecular structure for the organotellurium compounds was investigated using optimization plus frequency at the ground state level. In addition, density functional theory has been applied to optimize the

organotellurium compounds with Gaussian 09 software program [17,29-30] (see Fig. S13–S28).

HOMO (Highest Occupied Molecular Orbital) and LUMO (Lowest Unoccupied Molecular Orbital) energies are the electronic states, referring to certain places of the existence of the electrons with quantized energies, where the molecular orbitals are in linear combination to the atomic orbitals [17,30-31] (see Fig. S21–S28). The difference between HOMO provides the energy bandgap ( $E_g$ ). The energy gap is a crucial property in solids as it allows the prediction of the material (whether it is a conductor, insulator, or semiconductor). Furthermore, it represents the energy difference between the lower virtual energy and the higher total energy levels [32-34] (see Fig. S21–S28 and Table 3).

$$E_g = E_{\text{LUMO}} - E_{\text{HOMO}} \quad (1)$$

In the present work, a comparison between the HOMO and LUMO energies is explained in Table 3. to find out that HOMO energy of organyl tellurium dibromide A and C compound where is C a greater than D compound, as, for diorganyl telluride B and D, D is higher than C compound [32-34]. as follows:

$$D > B > A > C$$

Therefore, the highest energy gap was observed by compound D, while the lowest value was observed by compound C (see Table 3 and Fig. S21–S28).

### Electronegativity and electrophilicity

Electronegativity and electrophilicity can be calculated from [30,32-36] the relations 2 and 3 (see Table 4).

$$x = \frac{E_{\text{HOMO}} + E_{\text{LUMO}}}{2} \quad (2)$$

$$w = \frac{x^2}{2\eta} \quad (3)$$

In Table 4, the electronegativity of D was higher than the electronegativity of C and A. On the other hand, the electronegativity of compound B was the lowest.

$$D > C > A > B$$

Among the prepared compounds, compound B had the greatest electrophilicity, whereas compound D had the least.

$$B > A > C > D$$

### Ionization potential and electron affinity

According to Koopman's theory, the following relations, 4 and 5 [29-30,37], can express the ionization potential and electron affinity, as shown in Table 5.

$$\text{I.P} = -E_{\text{HOMO}} \quad (4)$$

$$\text{E.A} = -E_{\text{LUMO}} \quad (5)$$

Table 5 demonstrates the ionization potential, and electron affinity values in (eV) for compounds A, B, C, and D. According to Koopman's theorem, the ionization potential, and electron affinity results depend on the energies in the valence band and the conduction band. The table demonstrates the arrangement of the prepared compounds according to the increase in their ionization potential [29,37]:

$$B > D > A > C$$

### Hardness softness acid base (HSAB Principle)

The following equations 6 and 7 can express the hardness and softness [18,29,35,38]:

**Table 3.** The electronic states of the organotellurium compounds

Compound	HOMO (eV)	LUMO (eV)	$E_g$ (eV)
A	-3.795	-1.950	1.845
B	-7.438	-5.519	1.910
C	-3.565	-1.820	1.740
D	-4.549	-0.639	3.910

**Table 4.** Electronegativity and electrophilicity of the organotellurium compounds

Compound	Electronegativity (eV) (X)	Electrophilicity (eV) (w)
A	-2.87	4.44
B	-6.47	21.76
C	-2.69	4.12
D	-2.58	1.66

**Table 5.** Ionization potential and electron affinity of the organotellurium compounds

Compound	Ionization potential (eV) (I.P)	Electron affinity (eV) (E.A)
A	3.79	1.95
B	7.43	5.52
C	3.56	1.82
D	4.55	0.64

**Table 6.** Chemical hardness and chemical softness of the organotellurium compounds

Compound	Chemical hardness ( $\eta$ )	Chemical softness ( $\sigma$ )
A	0.92	0.54
B	0.95	0.52
C	0.87	0.57
D	1.96	0.25

$$\eta = \frac{I.P - E.A}{2} \quad (6)$$

$$\sigma = \frac{1}{2\eta} \quad (7)$$

$\eta$  refers to chemical hardness, and  $\sigma$  refers to chemical softness (see Table 6).

The comparison between A, B, C, and D shows that compound D was harder than compounds B, C, and A, respectively, indicating that compound D will behave as a hard base [29,35,38].

$D > B > C > A$

On the other hand, compound D was softer than compounds A, B, and C, indicating that compound C will behave as a soft base. Therefore, according to Table 6, the behavior of organotellurium compounds can be classified as donors or acceptors.

$C > A > B > D$

## ■ CONCLUSION

In the present study, compounds A, B, C, and D were obtained in a 51–65% yield. All the prepared compounds were characterized by the CHN elemental analysis, FTIR, and <sup>1</sup>H-NMR. Findings from this study were in concordance with previous research findings, confirming the correctness of the proposed structures for all the prepared compounds. Additionally, it is evident that the density functional theory used in this study was a powerful method, and B3LYP functional is a suitable and efficient function for studying the electronic properties of these structures.

## ■ REFERENCES

- [1] Al-Rubaie, A.Z., Al-Salim, N.I., and Al-Jadaan, S.A.N., 1993, Synthesis and characterization of new organotellurium compounds containing an *ortho*-amino group, *J. Organomet. Chem.*, 443 (1), 67–70.
- [2] Al-Rubaie, A.Z., Al-Masoudi, W.A., Al-Jadaan, S.A.N., Jalbout, A.F., and Hameed, A.J., 2008, Synthesis, characterization, and computational study of some new organotellurium compounds containing azomethine groups, *Heteroat. Chem.*, 19 (3), 307–315.
- [3] Yamago, S., 2021, Practical synthesis of dendritic hyperbranched polymers by reversible deactivation radical polymerization, *Polym. J.*, 53 (8), 847–864.
- [4] Al-Saadawy, N.H., 2021, Synthesis, characterization and theoretical studies of new organotellurium compounds based on (4-(((1S,E)-1,7,7-trimethyl bicyclo[2.2.1]heptan-2-ylidene)amino)phenyl) mercury(II) chloride, *Indones. J. Chem.*, 21 (6), 1443–1453.
- [5] Yousif, T.Y., 2020, Preparation of some new organotellurium compounds derived from 4,4-dihydroxy azobenzene, *Coll. Basic Educ. Res. J.*, 16 (3), 892–898.
- [6] Carrera Boutzis, E.I., 2017, Synthesis, Reactivity, and Photochemistry of  $\pi$ -Conjugated Tellurophenes, *Dissertation*, Department of Chemistry, University of Toronto, Canada.
- [7] Aziz, F.K., Gazar, S.H., and Al-Saadawy, N.H., 2020, Simple, selective, and sensitive spectrophotometric method for determination of trace amounts of lead(II), cadmium(II), cobalt(II) with organomercury compounds, *J. Global Pharma Technol.*, 12, 248–255.
- [8] Al-Asadi, R.H., 2020, Synthesis and molecular structure study of new organotellurium and organomercury compounds based on 4-bromonaphthalen-1-amine, *Russ. J. Gen. Chem.*, 90 (9), 1744–1749.
- [9] Ahmed, W.M., Al-Saadawy, N.H., and Abowd, M.I., 2021, Synthesis and characterization of a new organoselenium and organotellurium compounds depending on 9-chloro-10-nitro-9,10-dihydroanthracene, *Ann. Romanian Soc. Cell Biol.*, 25 (4), 11035–11043.

- [10] Kadhim, M.A., and Al-Saadawy, N.H., 2021, Synthesis and characterization for some new organoselenium compounds depending on 8-hydroxyquinoline, *Ann. Romanian Soc. Cell Biol.*, 25 (2), 2162–2172.
- [11] Al-Saadawy, N.H., 2022, New organotellurium compounds based on camphor, aniline and *p*-toluidine: Preparation, characterization and theoretical study, *Egypt. J. Chem.*, 65 (2), 19–27.
- [12] Pop, A., Silvestru, C., and Silvestru, A., 2019, Organoselenium and organotellurium compounds containing chalcogen-oxygen bonds in organic synthesis or related processes, *Phys. Sci. Rev.*, 4 (5), 20180061.
- [13] Pop, A., Silvestru, C., and Silvestru, A., 2019, "3. Organoselenium and Organotellurium Compounds Containing Chalcogen-Oxygen Bonds in Organic Synthesis or Related Processes" in *Selenium and Tellurium Reagents*, Eds. Laitinen, R., and Oilunkaniemi, R., De Gruyter, Boston, 61–122.
- [14] Tanini, D., and Capperucci, A., 2020, Unexpected ethyltellurenylation of epoxides with elemental tellurium under lithium triethylborohydride conditions, *Chemistry*, 2 (3), 652–661.
- [15] Tanini, D., and Capperucci, A., 2019, Ring-opening reactions of heterocycles with selenium and tellurium nucleophiles, *New J. Chem.*, 43 (29), 11451–11468.
- [16] Irfan, M., Rehman, R., Razali, M.R., Ur Rehman, S., Ur Rehman, A., and Iqbal, M.A., 2020, Organotellurium compounds: An overview of synthetic methodologies, *Rev. Inorg. Chem.*, 40 (4), 193–232.
- [17] Al-Asadi, R.H., 2019, Synthesis, DFT calculation and biological activity of some organotellurium compounds containing azomethine group, *Orbital: Electron. J. Chem.*, 11 (7), 402–410.
- [18] Panda, A., and Behera, R.N., 2014, Comparative study of E...N (E=Se/Te) intramolecular interactions in organochalcogen compounds using density functional theory, *J. Hazard. Mater.*, 269, 2–8.
- [19] Diki, N.Y.S., Coulibaly, N.H., Kambiré, O., and Trokourey, A., 2021, Experimental and theoretical investigations on copper corrosion inhibition by cefixime drug in 1 M HNO<sub>3</sub> solution, *J. Mater. Sci. Chem. Eng.*, 9, 11–28.
- [20] Zhang, Z., Hu, M., Zhang, W., and Zhang, X., 2022, Construction of tellurium-doped mesoporous bioactive glass nanoparticles for bone cancer therapy by promoting ROS-mediated apoptosis and antibacterial activity, *J. Colloid Interface Sci.*, 610, 719–730.
- [21] Arora, A., Oswal, P., Rao, G.K., Kumar, S., Singh, A.K., and Kumar, A., 2021, Tellurium-ligated Pd(II) complex of bulky organotellurium ligand as a catalyst of Suzuki coupling: First report on in situ generation of bimetallic alloy 'telluropalladinite' (Pd<sub>9</sub>Te<sub>4</sub>) nanoparticles and role in highly efficient catalysis, *Catal. Lett.*, 1–13.
- [22] Behera, R.N., and Panda, A., 2012, Nature of the Te...N intramolecular interaction in organotellurium compounds. A theoretical investigation by NBO and AIM methods, *Comput. Theor. Chem.*, 999, 215–224.
- [23] Kerbadou, R.M., Hadjadj Aoul, R., Benmaati, A., Taleb, A., Hacini, S., and Habib Zahmani, H., 2021, Identification of new biologically active synthetic molecules: Comparative experimental and theoretical studies on the structure-antioxidant activity relationship of cyclic 1,3-ketoamides, *J. Mol. Model.*, 27 (4), 109.
- [24] Silverstein, R.M., and Bassler, G.C., 1962, Spectrometric identification of organic compounds, *J. Chem. Educ.*, 39 (11), 546.
- [25] Bennett, A.J., Duke, C.B., and Silverstein, S.D., 1968, Theory of the tunneling spectroscopy of collective excitations, *Phys. Rev.*, 176 (3), 969.
- [26] Guthrie, R.D., 1978, Introduction to Spectroscopy (Pavia, Donald; Lampman, Gary M.; Kriz, George S., Jr.), *J. Chem. Educ.*, 56 (10), A323.
- [27] Scheinmann, F., 2013, An Introduction to Spectroscopic Methods for the Identification of Organic Compounds: Mass Spectrometry, Ultraviolet Spectroscopy, Electron Spin Resonance Spectroscopy, Nuclear Magnetic Resonance Spectroscopy (Recent Developments), Use of

- Various Spectral Methods Together, and Documentation of Molecular Spectra, Elsevier Science, Amsterdam, Netherlands.
- [28] Pavia, D.L., Lampman, G.M., Kriz, G.S., and Vyvyan, J.A., 2014, Introduction to Spectroscopy, Cengage Learning, Boston, US.
- [29] Oliveira, G.P., Barboza, B.H., and Batagin-Neto A., 2022, Polyaniline-based gas sensors: DFT study on the effect of side groups, *Comput. Theor. Chem.*, 1207, 113526.
- [30] Gusakova, J., Wang, X., Shiao, L.L., Krivosheeva, A., Shaposhnikov, V., Borisenko, V., Gusakov, V., and Tay, B.K., 2017, Electronic properties of bulk and monolayer TMDs: Theoretical study within DFT framework (GVJ-2e method), *Phys. Status Solidi A*, 214 (12), 1700218.
- [31] Fernandes, G.F.S., Pontes, M.A.P., Machado, F.B.C., and Ferrão, L.F.A., 2022, Electronic structure and stability of transition metal acetylacetonates  $\text{TM}(\text{AcAc})_n$  (TM = Cr, Fe, Co, Ni, Cu; n = 1, 2, 3), *Comput. Theor. Chem.*, 1207, 113502.
- [32] Xavier, R.J., and Gobinath, E., 2012, FT-IR, FT-Raman, *ab initio* and DFT studies, HOMO-LUMO and NBO analysis of 3-amino-5-mercapto-1,2,4-triazole, *Spectrochim. Acta, Part A*, 86, 242–251.
- [33] Arivazhagan, M., Manivel, S., Jeyavijayan, S., and Meenakshi, R., 2015, Vibrational spectroscopic (FTIR and FT-Raman), first-order hyperpolarizability, HOMO, LUMO, NBO, Mulliken charge analyses of 2-ethylimidazole based on Hartree-Fock and DFT calculations, *Spectrochim. Acta, Part A*, 134, 493–501.
- [34] Sheela, N.R., Muthu, S., and Sampathkrishnan, S., 2014, Molecular orbital studies (hardness, chemical potential, and electrophilicity), vibrational investigation and theoretical NBO analysis of 4-4'-(1H-1,2,4-triazol-1-yl methylene) dibenzonitrile based on *ab initio* and DFT methods, *Spectrochim. Acta, Part A*, 120, 237–251.
- [35] Vennila, P., Govindaraju, M., Venkatesh, G., and Kamal, C., 2016, Molecular structure, vibrational spectral assignments (FT-IR and FT-RAMAN), NMR, NBO, HOMO-LUMO and NLO properties of O-methoxybenzaldehyde based on DFT calculations, *J. Mol. Struct.*, 1111, 151–156.
- [36] Muya, J.T., Donald, K.J., Ceulemans, A., and Parish, C., 2021, A comparison of the chemical bonding and reactivity of  $\text{Si}_8\text{H}_8\text{O}_{12}$  and  $\text{Ge}_8\text{H}_8\text{O}_{12}$ : A theoretical study, *J. Chem. Phys.*, 154, 164305.
- [37] Vikramaditya, T., and Lin, S.T., 2017, Assessing the role of Hartree-Fock exchange, correlation energy and long-range corrections in evaluating ionization potential, and electron affinity in density functional theory, *J. Comput. Chem.*, 38 (21), 1844–1852.
- [38] Xu, H., Xu, D.C., and Wang, Y., 2017, Natural indices for the chemical hardness/softness of metal cations and ligands, *ACS Omega*, 2 (10), 7185–7193.